

Z. RANACHOWSKI\*<sup>‡</sup>, D. JÓŹWIAK-NIEDŹWIEDZKA\*, P. RANACHOWSKI\*, M. DĄBROWSKI\*, S. KUDELA JR.\*\* , T. DVORAK\*\*

**THE DETERMINATION OF DIFFUSIVE TORTUOSITY IN CONCRETE SPECIMENS USING X-RAY MICROTOMOGRAPHY**

**WYZNACZANIE KRĘTOŚCI DYFUZYJNEJ W PRÓBKACH BETONÓW PRZY ZASTOSOWANIU METODY MIKROTOMOGRAFII RENTGENOWSKIEJ**

The paper presents a method of pore connectivity analysis applied to specimens of cement based composites differing in water to cement ratio. The method employed X-ray microtomography (micro-CT). Microtomography supplied digitized three-dimensional radiographs of small concrete specimens. The data derived from the radiographs were applied as an input into the application based on the algorithm called 'random walk simulation'. As the result a parameter called diffusive tortuosity was established and compared with estimated porosity of examined specimens.

*Keywords:* X-ray tomography, concrete microstructure, diffusive tortuosity

Artykuł prezentuje metodę wyznaczania parametru charakteryzującego intensywność połączeń mikroporów w zastosowaniu do próbek kompozytów z matrycą cementową, różniących się stosunkiem wodnocementowym. Metoda bazuje na wynikach badań z zastosowaniem mikrotomografii rentgenowskiej. Analizowano zdigitalizowane zestawy danych, opisujące trójwymiarową reprezentację mikrostruktury niewielkich próbek wykonanych z betonu. Przygotowane w ten sposób skany mikrostruktury zastosowano jako dane wejściowe wprowadzone do oprogramowania wykorzystującego algorytm 'przypadkowo migrujących cząstek wirtualnych'. W ten sposób wyznaczono parametr mikrostruktury znany jako krętość dyfuzyjna. Parametr ten porównano z porowatością obserwowaną wyznaczoną dla zbadanych próbek przy wykorzystaniu analizy jasności voxelów w analizowanych próbkach.

**1. Introduction**

The research on durability of concrete outdoor structures is closely related to their properties of transport of potentially harmful ionic fluids and aggressive gases. The properties mentioned above strongly depend on the morphology of the pores inside the described material. In last years the micro-CT method was widely applied to get 3D digitized data sets useful to study on variety of issues related with concrete microstructure and its evolution due to ageing processes [1,2]. Fig. 1 presents examples of microstructure obtained with the application of micro-CT method of two brittle matrix composites extremely differing with their property of pore interconnectivity. The 3D images present a cubes of 3×3×3 mm reconstructed with the resolution of 5 μm per voxel (volumetric pixel).

Several authors applied the micro-CT technique in their research of concrete. The authors of present paper compared the average mortar density and volumetric pore distribution of three different concretes in [2] (2014). Garboczi [3] (2002) applied the micro-CT technique to reconstruct the aggregate shapes. He investigated concrete 108×108×108 mm cubes with voxel resolution of 0.4 mm<sup>3</sup>. The data obtained from the scans of the concrete samples enabled the author to approximate the real shapes of the recognized aggregates by its

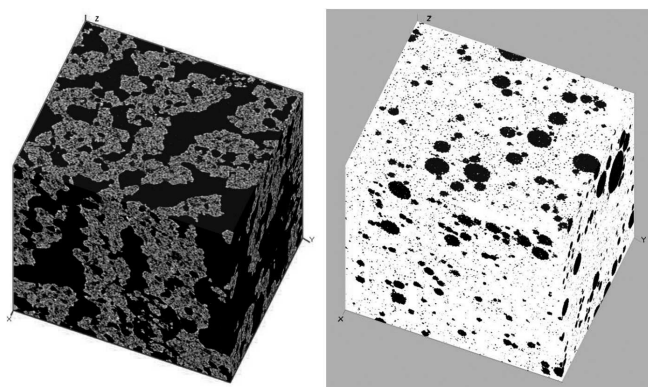


Fig. 1. Examples of microstructure obtained with the application of micro-CT method of two brittle matrix composites. Left: amorphous open-pore system formed in porous matrix of starch (intersection of baked bread); Right: spherical closed-pore system in tight cement paste matrix. The black regions denote voids and the bright regions are projections of dense phases (reconstructions made on the basis of microtomograms processed by the authors of present paper)

mathematical models to built the stereological model of entire population of aggregates. Lanzón et al. [4] (2012) used the

\* INSTITUTE OF FUNDAMENTAL TECHNOLOGICAL RESEARCH, POLISH ACADEMY OF SCIENCES, 5B, PAWIŃSKIEGO STR., 02-106 WARSZAWA, POLAND

\*\* INSTITUTE OF MATERIALS AND MACHINE MECHANICS, RACIANSKA 75, 831-02 BRATISLAVA, SLOVAKIA

‡ Corresponding author: zranach@ippt.pan.pl

micro-CT method to test the specimens made with crushed limestone aggregate (82.80 wt.%), cement CEM II/B-L 42.5R (16.50 wt.%) and additions (0.60 wt.%). Three low-density additions significantly different in parameters of their granulometric features have been used, i.e. their medians and variation coefficients were different. The low-density additions were: expanded perlite, expanded glass and cenospheres (hollow microspheres). The scanning was performed on cylinders of 8 mm in diameter and of 8 mm of height cut off the bulk of the mortars. The resolution of  $8 \mu\text{m}^3$  per voxel was achieved in resulting tomograms. The authors have determined capillary water absorption for mortars with the three different low-density additions and for the reference mortar by partial immersion of the samples in water. The results agreed with the volumetric pore concentration data obtained by processing of test results using micro-CT. The correlation coefficient of 0.964 was obtained between the air pores content determined using micro-CT and the capillary water absorption. That nature of the mortars allows for precise segmentation of air pores since air is clearly differentiated from the solid and gelled components. Stock et. al. [5] (2002) analysed the progression of sulfate attack within the cement paste. In the paper they presented the microstructure of their specimens. The specimens were the cylinders of 10 mm diameter and of 40 mm length. The resolution of rendered images was 20  $\mu\text{m}$  in cross-sections and 30  $\mu\text{m}$  in thickness. The recognized damage levels in specimens exposed to a  $\text{Na}_2\text{SO}_4$  solution in different conditions varied from 0 (no damage) to 4 (extreme damage). Nakashima and Kamia [6] (2012) derived transport properties (i.e.: segmented porosity, surface to volume ratio of pores and diffusion tortuosity of recognized pore system) in investigated porous rock piece. The algorithm of determining of diffusion tortuosity is described in more details in the next paragraph of the present paper as a major goal of the present research. The authors have investigated a cylindrical sample of 7.5 mm in diameter and of 8.1 mm. The image resolution was  $15 \mu\text{m}^3$  per voxel. Provis et al. [7] (2012) tested the mixes of cement and siliceous fly ash and ground granulated blast furnace slag in different proportions after the ageing period of 4, 8, 16 and 48 days. The scanning was performed on agglomerates of particles of approx.  $1 \times 1 \times 1$  mm with application of radiation from the high-energy synchrotrone source. Due to the use of high resolution detector a resolution of  $0.75 \mu\text{m}^3$  at the tomograms was achieved. The aim of investigation was to trace the volume evolution of pores and to determine the time changes of connectivity within the pore system. To characterise the connectivity of pores a diffusion tortuosity was determined in similar way that in [7]. The authors concluded that the latter parameter configuration could be applied as a measure of a susceptibility of cement binders to migration processes of aggressive media causing structural damages.

The tools for material testing with micro-CT technique are produced at present by a few firms and are capable to perform tests on the small specimens of few millimeters size or on large elements of a few meters. They include the microfocal source of X-ray radiation, the movable table to place a specimen, and the flat panel with a square high resolution radiation detector. The structure of concrete is visualized on the cross-sections (tomograms) of the investigated specimen the using 0.255/8 bit grey scale convention related directly

to the amount of local radiation absorption of the material. The grey scale is ordered from white related to maximum of absorption to black related to the minimum, respectively.

Unhydrated cement particles and aggregate grains are objects of the greatest absorption. The hydration products that cover major part of the cement matrix present slightly lower absorption ability. The next in the line are hydrated calcinates and at the end of the scale are the regions of high porosity. With application of micro-CT technique it is possible to reconstruct a real 3-dimensional image of investigated microobjects and to determine the volumetric part of the material occupied by bulk matrix, aggregates, voids, pores, cracks, etc. with resolution of some micrometers<sup>3</sup> per voxel. It is also possible to improve the image resolution as it was described by Gallucci [8].

A specimen for micro-CT testing should be extracted from the investigated concrete specimen by drilling out a core with diameter  $\sim 10$  mm. The scanning procedure lasts approximately 1 hour and does not require any special processing of the surface of tested specimen. The method is particularly useful to deliver rapid though not extremely precise microstructural parameters of the investigated concrete; sometimes sufficient for comparative tests. Since the flat panel detectors usually represent the resolution of  $2000 \times 2000$  pixels, it may be concluded that the effective image resolution is one promille of the greater specimen dimension and that is why the specimen dimensions cannot exceed a few millimeters. Digitizing the images of microstructure enables for merging the data obtained from several specimens into one set of data. The limitation of dimensions is the argument to limit to the matrix without coarse aggregate grains.

## 2. The algorithm of determining of diffusive tortuosity

The process of digitizing of the concrete specimens results in binary datasets of consecutive crosssections. The authors of present paper have obtained 1800 crosssections (reconstructed every 5  $\mu\text{m}$  of specimen height),  $2000 \times 2000$  of pixels each as a result of scanning of a  $\Phi 9 = \text{mm}$  and  $H = 9$  mm cylinder with an resolution of  $5 \mu\text{m}^3$  per voxel. With the coding scheme of 1 byte per pixel, the total number of bytes in such a dataset would be 7,200,000,000 bytes. It is inconvenient to be processed in one piece in computer memory. To make the image processing possible the usual procedure used by the majority of the authors cited, is to extract a subset of data, preferably of cubic shape for further computations. The resulting subset is called a ROI (Region Of Interest) and is immune from the cracked areas situated in proximity of the specimen surface usually damaged by a drilling tool. The authors of [7] analysed ROIs containing  $255^3$  voxels. In [8]  $1000^3$  voxels were processed. The authors of present paper decided to process 6 different ROIs of  $600^3$  (216,000,000) voxels each. That way the ROIs described in next paragraphs represented cubes of  $3 \times 3 \times 3$  mm. To analyse the internal pore network connectivity a random walk algorithm [7] was implemented in a form of originally prepared executable program for the PC computer. The latter algorithm originally was intended to simulate the diffusion of gases and liquids in the interconnected network of pores. At the starting point of the

action a certain number of ‘walkers’ was distributed randomly across the space reconstructed by means of the micro-CT scanning procedure. The ‘walkers’ occupy one voxel of space and can be understood as a marked point in the dataset representing the analysed volume of the specimen. The walkers migrated on neighbouring voxels obeying the information on voxels brightness (i.e. material density). The walkers executed jumps in randomly chosen direction but the jumps could be performed if the neighbouring voxel belonged to a pore and otherwise the jumps were discarded. After refreshing the position of all walkers, one epoch of its action was completed by the algorithm. The number of epochs was measured by the dimensionless integer time  $t$ . The primary output of the random walk procedure is the walkers mean-square displacement  $\langle r(t)^2 \rangle$  as a function of time ( $x_i, y_i, z_i$  are the coordinates of a current walker position and  $n$  is a number of operating walkers):

$$\langle r(t)^2 \rangle = \frac{1}{n} \sum_{i=1}^n [(x_i(t) - x_i(0))^2 + (y_i(t) - y_i(0))^2 + (z_i(t) - z_i(0))^2] \quad (1)$$

The key transport property called diffusion tortuosity  $\tau$  of the porous medium is related to the time-derivative of  $\langle r(\tau)^2 \rangle$  and can be expressed as:

$$\tau = \frac{A}{d \langle r(\tau)^2 \rangle / dt} \text{ as } t \rightarrow \infty \quad (2)$$

where  $A$  is a constant depended of implemented image lattice parameters and by some authors [7,8] is assumed as 1.

The way of determining of  $\tau$  as a converging limit of  $d \langle r(\tau)^2 \rangle / dt$  needs the explanation. As time  $t$  elapsed random walkers migrated in porous media further than the average pore size. In the long - time limit they experienced the *tortuosity* of the surrounding material and the slope of  $\langle r(\tau)^2 \rangle$  reached a constant value. Hence, the tortuosity is defined by (2). In practical condition to determine the slope  $d \langle r(\tau)^2 \rangle / dt$  a one uses a procedure performing the calculation of the statistical coefficient of a least-squares linear regression using the consecutive 100 values of  $\langle r(\tau)^2 \rangle$  taken for the large values of  $t$ . According to the assumptions found in [8] the authors of present paper have tested 6000 walkers and the slope of  $d \langle r(\tau)^2 \rangle / dt$  was checked in the proximity of  $t = 400,000$  (i.e. for  $t = 399100, 399101$  and so on...) for ten times. The resulting value of diffusive tortuosity was calculated as the average of the obtained results for which the correlation coefficient of the linear regression procedure was greater than 0.8. The diffusive tortuosity is an indirect function of the porosity of the body. The Fig. 2. below presents two model structures characterised by the volume fraction of

porosity equalled 1%. The porosity is represented by the rectangular channel crossing the central part of both structures. At the left side of the figure the channel possesses continuing interior and at the right side the channel is divided approx. into two halves by the thin obstacle. The tortuosity calculated with the program described in present paragraph resulted in a value of 28 in the case of the long channel and in a value of 56 for the obstructed variant, respectively.

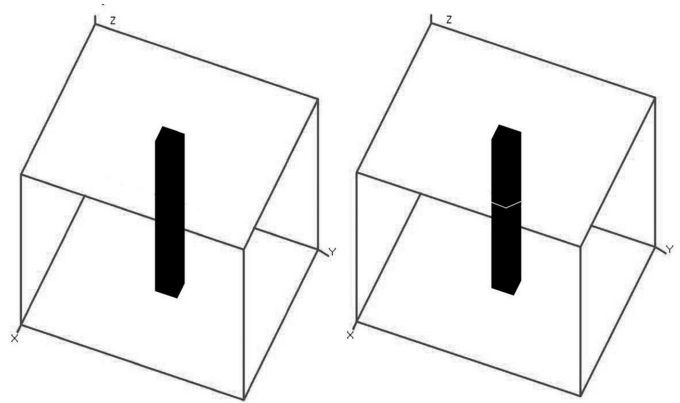


Fig. 2. An example of two model structures, representing the same volume fraction of porosity (black part of the cube), used for testing of prepared procedure for calculating of the tortuosity. The rectangular channel crossing the central part left structure has no discontinuities and at the right side the channel is divided into two halves by the thin obstacle

### 3. Experimental

Three concrete mixes were designed and prepared of the same ingredients but with different water to cement ratio to result in different level of porosity. Sand of fraction 0-2 mm as fine aggregate and crushed amphibolite of fractions 2-8 and 8-16 mm as coarse aggregate were used. The composition of concrete mixes is shown in Table 1.

The beams 100×100×500 mm were cast for testing of progress of carbonation and stored for 27 days in water at temperature of +22°C. Then they were stored at laboratory conditions at +20°C, 60% RH until the mass equilibrium was reached (14 days).

Micro-CT method was applied with Nanotom 30 microtomograph made by General Electric operating in the Institute of Materials and Machine Mechanics in Bratislava. The space resolution of the reconstructed microstructure was  $5 \mu\text{m}^3$  per voxel.

TABLE 1

Composition of tested concretes, kg/m<sup>3</sup>

Mix designation	cement CEM I 42.5 R	fine aggregate 0-2 mm	coarse aggregate 2-8 mm	coarse aggregate 8-16 mm	water	superplasticizer, % cement mass	Mix specific density [kg/m <sup>3</sup> ]
A	350	630	695	655	158	0.30	2424
B	400	580	625	615	200	0.00	2433
C	320	630	675	650	176	0.00	2431

The result of micro-CT scanning was a set of tomograms (specimen cross-sections), performed every 5 μm along the specimen height. The digitized form of tomograms characterized the microstructure of specimens and included the information about the material in form of values of brightness in arbitrary units [a.u.] for all pixels of extracted specimen piece. Voxel brightness was proportional to the local density of the material. Two data subsets (ROIs) were extracted from the datasets representing the specimens. The ROIs labelled A1, B1 and C1 characterized with cement matrix to aggregate ratio of ca. 40% are presented of Fig. 3.

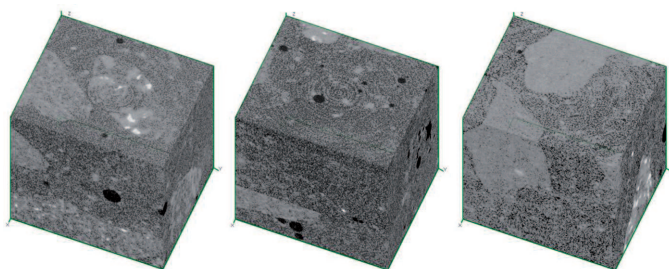


Fig. 3. The ROIs labelled A1, B1 and C1 prepared of specimen parts characterized with cement matrix to aggregate ratio of ca. 40%

To determine the impact of cement matrix amount to the results of calculating of tortuosity, the other group, labelled A2, B2 and C2 was prepared in such a way to obtain cement matrix to aggregate ratio of ca. 30% what is depicted in Fig. 4.

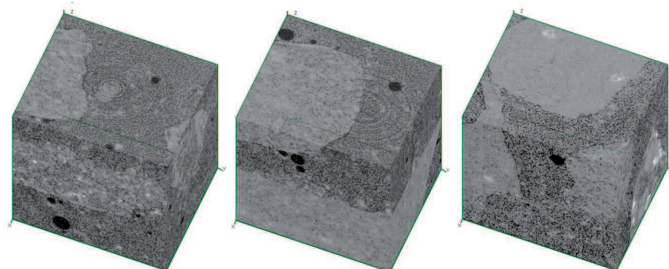


Fig. 4. The ROIs labelled A2, B2 and C2 prepared of specimen parts characterized with cement matrix to aggregate ratio of ca. 30%

In order to determine magnitudes of brightness of voxels belonging to pores, cement matrix and aggregates greyscale value histograms were performed for ROIs presented in Figs 3. and 4. These histograms are presented in Fig. 5.

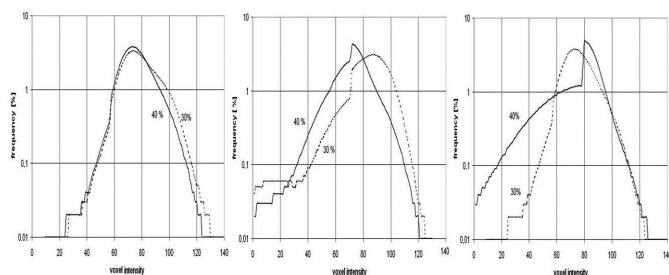


Fig. 5. Greyscale value histograms for the all ROIs examined in the paper (left: specimen A, center: specimen B and right : specimen C, the labels denote the cement matrix to aggregate ratio of the ROI)

In a part of the histograms presented in Fig. 5 one can mention distinct discontinuities at histogram curves resulted

by the transition from one material phase to another (i.e. pores->matrix-> aggregates) what was discussed in [8]. It is obvious that the magnitude of the discontinuities depends on the volume distribution of phases in investigated piece of the material. Assuming the information which was derived from the greyscale histograms presented above the authors of the paper decided to take the following average brightness levels to distinguish the phases within analysed ROIs: 40 as the pores-matrix transition and 70 as the matrix-aggregates transition. It was proven that the variations made on these levels in magnitude of 2 or 4 percent have little influence for further determination of microstructural parameters.

After the determination of greyscale levels related to three principal material phases it was possible to process the prepared ROIs using the algorithm of random walk presented in previous chapter. The graphical illustration of the range of walkers migration in the ROIs of type 1. is presented in Fig. 6. The visualisation was made after 400,000 of time steps. The final positions of first 500 walkers are marked with small dots.

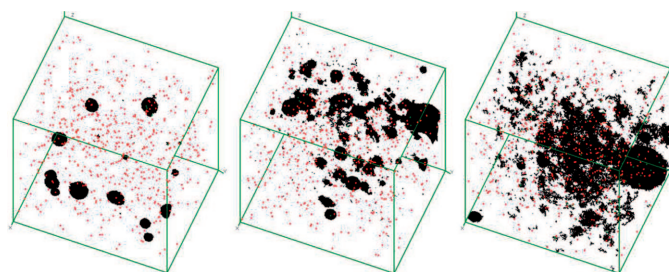


Fig. 6. Illustration of paths (depicted as black regions) taken by the walkers through the tortuous pore network of ROIs of type A1, B1 and C1. The procedure settings was 6000 walkers and 400,000 of time steps

TABLE 2

Parameters related to the porosity of the tested specimens, determined on the basis of the digital data by means of micro-CT method

material parameter	specimen A	specimen B	specimen C
water to cement ratio	0.45	0.5	0.55
pore volume to matrix volume in specimen part characterized with cement matrix to aggregate ratio of ca. 40%	0.8 %	4 %	18 %
pore volume to matrix volume in specimen part characterized with cement matrix to aggregate ratio of ca. 30%	0.8 %	2 %	17 %
diffusive tortuosity in specimen part characterized with cement matrix to aggregate ratio of ca. 40%	282	43	81
diffusive tortuosity in specimen part characterized with cement matrix to aggregate ratio of ca. 40%	244	96	46

For each ROI the ratio of pore volume to matrix volume was determined. The latter parameter called 'segmented

porosity' can be used to characterize the concrete microstructure. The results of the analysis of the data obtained from the specimens by means of micro-CT method are summarized in Table 2.

#### 4. Conclusions

The results of the investigation allow the authors to conclude that the micro-CT method is capable to deliver some information on the microstructure of tested concrete specimens after contactless and relatively fast inspection. The important point of the data analysis is the proper determination of the pores-matrix threshold and matrix-aggregates threshold in respect to the population of examined voxel brightness parameter. After the assumption of the latter parameter it is possible to determine the segmented porosity what is proportional to water to cement ratio and thus is proportional to the material porosity. It is also possible to calculate the diffusive tortuosity - the parameter describing the pore connectivity of the investigated material. However that parameter presents non-linear dependence on segmented porosity as it was discussed in [8] because it is sensitive to the configuration of pore system. The authors of this paper have determined the close related results of diffusive porosity for specimens with w/c parameter of 0.5 and 0.45 but this parameter was of significant different magnitude for specimen with higher w/c ratio. The procedure of determining of diffusive porosity resulted in a relatively large deviation of results and perhaps need more repetitions. However it is evident that combined with the derived value of segmented porosity can be a fast tool for determining of microstructural parameters of concrete in some applications.

#### Acknowledgements

The results presented in the paper have been obtained within the Joint Project of Polish and Slovak Academies of Sciences no. 10 en-

titled 'Investigation of novel concrete compositions with application of X-ray microtomography'.

#### REFERENCES

- [1] E. Landis, E. Nagy, D. Keane, S.P. Shah, Observations of internal crack growth in mortar using X-ray microtomography, Proc. of the Fourth Materials Engineering Conf. Washington, D.C., ASCE, New York (1996).
- [2] Z. Ranachowski, D. Józwiak-Niedźwiedzka *et al.*, Application of X-ray microtomography and optical microscopy to determine the microstructure of concrete penetrated by carbon dioxide, Archives of Metallurgy and Materials, 59,4, (2014) DOI: 10.2478/amm-2014-0245, 1451-1457.
- [3] E.J. Garboczi, Three-dimensional mathematical analysis of particle shape using X-ray tomography and spherical harmonics: Application to aggregates used in concrete, Cement & Concrete Research **32**, 1621-1638 (2002).
- [4] M. Lanzon, V. Cnudde, T. de Kock, J. Dewanckele, X-ray microtomography ( $\mu$ -CT) to evaluate microstructure of mortars containing low density additions, Cement & Concrete Composites **34**, 993-1000 (2012).
- [5] S.R. Stock, N.K. Naik, A.P. Wilkinson, K.E. Kurtis, X-ray microtomography (micro-CT) of the progression of sulfate attack of cement paste, Cement & Concrete Research **32**, 1673-1675 (2001).
- [6] Y. Nakashima, S. Kamia, Mathematica Programs for the Analysis of Three-Dimensional Pore Connectivity and Anisotropic Tortuosity of Porous Rocks using X-ray Computed Tomography Image data, J. of Nuclear Science and Technology **44**, 9, 1233-1247 (2012).
- [7] J.L. Provis, R.J. Myers, C.E. White, X-ray microtomography shows pore structure and tortuosity in alkali-activated binders, Cement & Concrete Research **42**, 855-864 (2012).
- [8] E. Gallucci, K. Scrivener, A. Groso, M. Stampanoni, G. Margaritondo, Experimental investigation of the microstructure of cement pastes using synchrotron X-ray microtomography ( $\mu$ CT), Cement & Concrete Research **37**, 360-368 (2007).